

# 134 Topics in Current Chemistry

## Analytical Problems

With Contributions by  
H. U. Borgstedt, H. W. Emmel, E. Koglin,  
R. G. Melcher, Th. L. Peters, J.-M. L. Séquaris

## Editorial Board

- Prof. Dr. *Michael J. S. Dewar* Department of Chemistry, The University of Texas  
Austin, TX 78712, USA
- Prof. Dr. *Jack D. Dunitz* Laboratorium für Organische Chemie der  
Eidgenössischen Hochschule  
Universitätsstraße 6/8, CH-8006 Zürich
- Prof. Dr. *Klaus Hafner* Institut für Organische Chemie der TH  
Petersenstraße 15, D-6100 Darmstadt
- Prof. Dr. *Edgar Heilbronner* Physikalisch-Chemisches Institut der Universität  
Klingelbergstraße 80, CH-4000 Basel
- Prof. Dr. *Shô Itô* Department of Chemistry, Tohoku University,  
Sendai, Japan 980
- Prof. Dr. *Jean-Marie Lehn* Institut de Chimie, Université de Strasbourg, 1, rue  
Blaise Pascal, B. P. Z 296/R8, F-67008 Strasbourg-Cedex
- Prof. Dr. *Kurt Niedenzu* University of Kentucky, College of Arts and Sciences  
Department of Chemistry, Lexington, KY 40506, USA
- Prof. Dr. *Kenneth N. Raymond* Department of Chemistry, University of California,  
Berkeley, California 94720, USA
- Prof. Dr. *Charles W. Rees* Hofmann Professor of Organic Chemistry, Department  
of Chemistry, Imperial College of Science and Technology,  
South Kensington, London SW7 2AY, England
- Prof. Dr. *Fritz Vögtle* Institut für Organische Chemie und Biochemie  
der Universität, Gerhard-Domagk-Str. 1,  
D-5300 Bonn 1
- Prof. Dr. *Georg Wittig* Institut für Organische Chemie der Universität  
Im Neuenheimer Feld 270, D-6900 Heidelberg 1

# Surface Enhanced Raman Scattering of Biomolecules

Eckhard Koglin and Jean-Marie Séguaris

Institute of Applied Physical Chemistry, Nuclear Research Center (KFA) Jülich, P.O. Box 1913,  
D-5170 Jülich/FRG

## Table of Contents

<b>1 Introduction</b>	<b>3</b>
<b>2 Experimental Features</b>	<b>4</b>
2.1 Electrode SERS	5
2.2 Colloid SERS	8
<b>3 Characteristics of SERS</b>	<b>10</b>
3.1 Raman Scattering of Adsorbates	10
3.2 The EM Model for SERS	12
3.3 The Chemical Effects in SERS	14
<b>4 Applications of SERS-Spectroscopy</b>	<b>15</b>
4.1 The Short-Range Sensitivity of SERS	15
4.2 Native DNA	20
4.2.1 DNA Bases	22
4.2.2 Mononucleotides	23
4.2.3 Double-Stranded Polynucleotides	25
4.3 Modified DNA	27
4.3.1 $\gamma$ -Radiation	27
4.3.2 Chemical Methylation	27
4.3.3 Temperature Effects on Native DNA	30
4.3.4 Pt-coordination Compounds	30
4.4 Micro-SERS of Chromosomes	31
4.5 Other Substances of Biochemical Significance	32
4.6 Amino Acids	36
4.7 Proteins	37

<b>5 Surface Enhanced Resonance Raman Scattering (SERRS)</b>	<b>40</b>
5.1 Porphyrin Chromophores	41
5.1.1 Water-Soluble Porphyrins	41
5.1.2 Bile Pigments	42
5.1.3 Metalloporphyrins	44
5.1.3.1 Hemin	44
5.1.3.2 Chlorophyll Pigments	46
5.1.4 Hemoproteins	48
5.1.4.1 Myoglobin	48
5.1.4.2 Cytochrome	48
5.2 Flavin Chromophores	50
5.3 Retinal Chromophore	51
<b>6 The Future</b>	<b>52</b>
<b>7 Acknowledgements</b>	<b>53</b>
<b>8 References</b>	<b>53</b>

A review of Surface Enhanced Raman Scattering (SERS) and Surface Enhanced Resonance Raman Scattering (SERRS) from biomolecules adsorbed on a metal surface is given. Advantages and applications of these new vibration spectroscopic methods particularly in characterize in-situ the chemical identity, structure, orientation, chemical and electrochemical reactions of biological specimens adsorbed at charged surfaces are discussed. The technical aspects of the instrumentation and procedure as also the fundamentals of the SERS theory are exposed. Different applications show that SERS- and SERRS spectroscopy are powerful in-situ methods to study the interfacial behaviour of biomolecules. Moreover, the high enhancement factor of the Raman scattering intensity creates a new technique for obtaining high resolution vibrational spectra of biomolecules from rather diluted aqueous solutions down to  $10^{-8}$  M.

# Analytical Problems

With Contributions by  
H. U. Borgstedt, H. W. Emmel, E. Koglin,  
R. G. Melcher, Th. L. Peters, J.-M. L. Séquaris

With 58 Figures and 16 Tables



Springer-Verlag  
Berlin Heidelberg New York Tokyo

This series presents critical reviews of the present position and future trends in modern chemical research. It is addressed to all research and industrial chemists who wish to keep abreast of advances in their subject.

As a rule, contributions are specially commissioned. The editors and publishers will, however, always be pleased to receive suggestions and supplementary information. Papers are accepted for "Topics in Current Chemistry" in English.

ISBN 3-540-16403-0 Springer-Verlag Berlin Heidelberg New York Tokyo  
ISBN 0-387-16403-0 Springer-Verlag New York Heidelberg Berlin Tokyo

This work is subject to copyright. All rights are reserved, whether the whole or part of the material is concerned, specifically those of translation, reprinting, re-use of illustrations, broadcasting, reproduction by photocopying machine or similar means, and storage in data banks. Under § 54 of the German Copyright Law where copies are made for other than private use, a fee is payable to "Verwertungsgesellschaft Wort", Munich.

© by Springer-Verlag Berlin Heidelberg 1986  
Printed in GDR

The use of registered names, trademarks, etc. in this publication does not imply, even in the absence of a specific statement, that such names are exempt from the relevant protective laws and regulations and therefore free for general use.

Typesetting and Offsetprinting: Th. Mützer, GDR;  
Bookbinding: Lüderitz & Bauer, Berlin  
2152/3020-543210

## 1 Introduction

The structure and dynamics of chemisorbed biomolecules are of great importance in order to elucidate the behaviour of these molecules at electrically charged surfaces. Recently, it has been suggested that Raman spectroscopy at solid/liquid interfaces becomes a general tool for the study of the physicochemical phenomena that take place in such environments<sup>1-8)</sup>. In his early overview on Surface Enhanced Raman Scattering (SERS) Van Duyne<sup>1)</sup> estimated that the expected scattering intensity from the adsorbed molecules is  $10^5$ – $10^6$  times stronger than for nonadsorbed species at the same bulk concentration. Such enormous enhancement totally overcomes the traditional low sensitivity problem associated with Normal Solution Raman Scattering (NSRS). This enables researchers to characterize *in-situ* the chemical identity, structure, orientation and chemical reactions of species adsorbed at surfaces applying SERS.

Today a rather detailed knowledge of the conformational changes of nucleic acids and proteins in the solution state is available with NSRS and this knowledge is continuously growing<sup>9-12)</sup>. On the other hand much less information exists about the interfacial behaviour of these biopolymers, due to the lack of suitable methods. However, the following important processes are typically interfacial:

- (I) control of the genetic information,
- (II) mechanisms of blood clotting,
- (III) redox enzymatic reactions at mitochondrial membranes.

In 1979, the SERS-spectroscopy was first applied to the study of adsorbed biopolymers in the case of nucleic acids<sup>13)</sup>. This was the starting signal for the rapid expansion of SERS into the field of biochemistry from the hitherto existing corner restricted to the investigation of some organic substances, predominantly pyridine derivatives, and some simple inorganic adsorbates.

Using biomolecules with chromophoric groups the Raman bands are both resonance (RRS) — and surface enhanced (RRS + SERS = SERRS). Instead of the usual term SERS, the Raman effect is, in this case, called surface enhanced resonance Raman scattering (SERRS). SERRS spectroscopy was first applied to biochemistry of heme chromophores by Cotton et al.<sup>14)</sup>. Since then, SERS and SERRS have been extended to systematic investigations of biomolecules in the adsorbed state<sup>15-41, 186-191)</sup>.

What is the advantage of SERS-spectroscopy in biological science? The high enhancement factor of the Raman scattering intensity by the adsorbed biomolecules creates a new technique for obtaining high resolution vibrational spectra of biomolecules from very diluted aqueous solutions down to  $10^{-8}$  M. This means that only very small amounts of material are needed, e.g. of compounds which are not available in large amounts, because they are difficult to prepare and hence very expensive and valuable. Recording the NSRS spectra of many biomolecules is impossible because of their very low solubility in water. However, vibration spectra of biomolecules with a solubility lower than  $5 \times 10^{-4}$  g in 100 g H<sub>2</sub>O have been obtained by means of SERS-spectroscopy<sup>25, 31, 41)</sup>. The decisive point of this new spectroscopic method was the distance of the Raman enhancement from the surface. The sterical investigations of the biopolymers DNA and poly-A adsorbed at positively charged silver surfaces (electrodes, colloids) have indicated that the sensitivity of the enhance-

ment is limited by the short-range enhancement to distances near the surfaces<sup>26,40</sup>. Thus, SERS-spectroscopy is a very sensitive method used to detect moieties of an adsorbed biopolymer situated close to a charged surface. The purpose of this contribution is to review the recent advances in the application of SERS- and SERRS spectroscopy in biological science.

## 2 Experimental Features

After the first detection of the enhanced Raman signals from pyridine adsorbed on a silver metal electrode<sup>42</sup>) it is now well established that this phenomenon is caused by an enhancement of the Raman cross section of adsorbates at an electrode-electrolyte interface<sup>42-68</sup>), on metal colloids<sup>69-93</sup>) and at a metal-vacuum surface<sup>94-98</sup>).

All investigators have outlined that "surface roughness" is a prerequisite for such an enhancement in the Raman scattering intensity. This roughness can be created by various types of processes: electrochemical<sup>2</sup>), chemical reduction<sup>69</sup>), mechanical polishing<sup>99</sup>), vapour deposition<sup>100</sup>), lithography<sup>94,101</sup>), evaporation<sup>102</sup>) and photochemical<sup>103</sup>). Metals, which have been successfully employed as substrates for SERS belong qualitatively into several groups.

i) Noble metals, e.g., Ag, Cu and Au, at which d-bands lie well below the Fermi level.

ii) Transition metals, e.g., Ni, Pd, Pt, of which d-bands overlap the Fermi level and thereby contribute to a strong covalent bonding of adsorbates.

iii) Metals, such as Al, Na and K, which do not have d-bands and are free-electron-like. Up to now SERS experiments with biomolecules are carried out only in an electrochemical cell with Ag electrodes or in a Ag colloid solution.

For the study of adsorbed biological, significant species a typical experimental arrangement is shown in Fig. 1. Generally for "Electrode SERS spectroscopy" a conventional three-electrode configuration is used, with the potentiostat maintaining the potential of the working electrode relative to the reference electrode and a function generator as programmer for the oxidation (dissolution) — reduction (deposition)

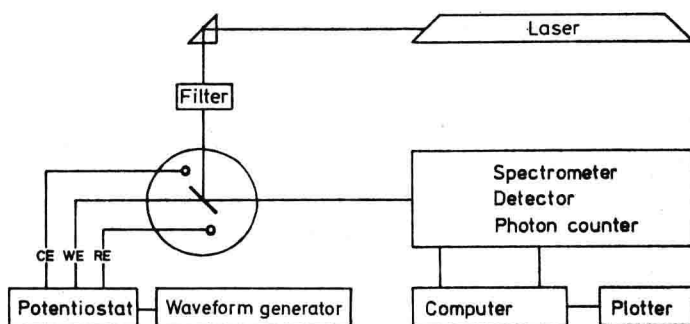


Fig. 1. Typical Raman spectroelectrochemistry equipment system. WE, working electrode; CE, counter electrode; RE, reference electrode



**Table 1.** Biomolecules investigated by SERS and SERRS

<b>Purine</b>	
Sugars:	Ribose, Deoxyribose
Nucleic Bases:	Adenine (A), Guanine (G), Cytosine (C), Thymine (C)
Nucleosides:	Adenosine, Guanosine, Cytidine, Uridine, Thymidine
Nucleotides:	(d)AMP, ADP, ATP, (d)GMP, (d)CMP, UMP, TMP
Dinucleoside Monophosphates:	ApA, ApC, ApG, ApU
Polynucleotides:	Poly A, Poly C, Poly U, Poly A · Poly U, Poly I · Poly C
Deoxyribopolynucleotides and Nucleic Acids:	Poly d(AT), Poly d(GC), Poly dG · Poly dC, Native and denatured DNA
Amino Acids:	Phenylalanine, Tryptophan, Tyrosine, Histidine, Glutamine, Glycine, Alanine
Aminobenzoic Acid:	p-Aminobenzoic Acid (PABA)
Citric Acid:	Sodium Citrate
Porphyrin Chromophores:	porphyrins, bile pigments, metalloporphyrins, hemoproteins
Flavin Chromophores:	Flavoproteins, glucose oxidase
Retinal Chromophore:	Bacteriorhodopsin

cycles (ORC). "Colloid SERS spectroscopy" is carried out with a conventional Raman cell for liquids or with capillary tubes. Most surface Raman spectra were measured using a computer controlled double monochromator with a cold photomultiplier, operated in the photon counting mode. The efficient optical system of the spectrometer is combined with a powerful laser light source.

A list of biomolecule adsorbates studied presently is given in Table 1. The number of materials investigated, however, grows rapidly. The activity in this field of SERS-spectroscopy is used for two types of Raman scatterers: laser excitation far removed from the electronic absorption maxima and excitation of species at wavelengths near to or at absorption maxima. SERS studies of species adsorbed on metal surfaces with absorption bands near the UV region (DNA and the derivatives, proteins without chromophoric groups) have shown that Raman signals can be enhanced by as much as  $10^4$ – $10^7$  fold<sup>19,25)</sup>. When combined with resonance Raman scattering from an appropriate chromophoric adsorbate, total Raman enhancement factors might reach values in the  $10^{10}$  to  $10^{12}$  range<sup>21,91)</sup>.

## 2.1 Electrode SERS

The electrochemical cells used for SERS studies on polycrystalline silver electrodes are shown in Fig. 2. In the spectroelectrochemical cell the Ag working electrode is placed in such a position that the laser light can be focused onto its surface and the backscattered light can then be efficiently collected. The optoelectrochemical cell is usually a quartz glass cylinder with a diameter of about 1.5 cm and a volume of 2 ml<sup>39)</sup>. The polycrystalline Ag working electrode is positioned in the center of the cell for optimal substance diffusion and electrochemical conditions (cf. Fig. 2a). The cell can be used in experiments where the angle of incidence is varied by rotating

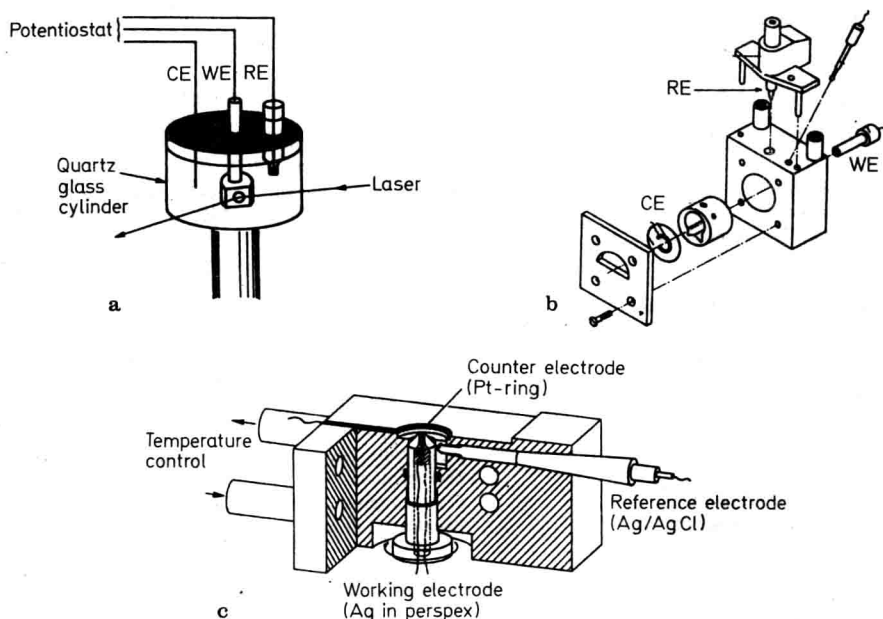


**Fig. 2a-c.** Raman spectroscopic cell designs for electrode surface studies: **a** Ervin et al., Ref. <sup>16)</sup>; **b** and **c** Otto et al., Ref. <sup>36)</sup>

the cell round the axis of the working electrode. In this cell design, the Raman scattering is measured at  $90^\circ$  to the incident laser radiation. The reference electrode in the cell is a Ag/AgCl electrode or a saturated calomel electrode (SCE). The third electrode of this three-electrode cell is simply a platinum wire as the counter electrode.

Surface enhanced Raman signals from the electrode can be observed using different pretreatment procedures:

a) The surface is pretreated by running the electrochemical oxidation-reduction cycle (ORC) in the bulk solution containing the biomolecules.

b) The electrode roughening procedure is carried out in the electrolyte solution in the absence of the biomolecule and the biomolecule solution is then added to the cell.

c) The silver electrode is removed from the cell after the electrochemical cycle, dried and the spectra are measured in air. One of the most important problems in the use of the SERS effect for the study of adsorbed conformations of nucleic acids, proteins and peptides is conservation of their conformational state during the ORC. Thus, to avoid conformational changes of the large biomolecules during the electrochemical cycle procedure (b) should be preferred.

A demonstration of the advantage of high sensitivity in SERS spectroscopy is given in Fig. 3. This figure displays the SERS spectrum of the DNA base cytosine <sup>39)</sup>. The laser power used to excite the sample was only 10 mW at 514.5 nm from an argon ion laser. An important observation is that the band positions obtained in SERS spectra are essentially the same as in NSRS spectra. The largest frequency shift

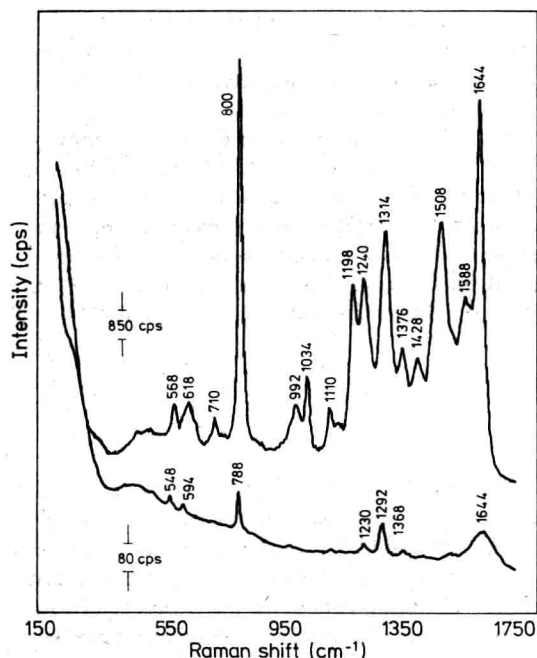


**Fig. 3.** SERS spectrum of cytosine (above). Conditions: laser excitation line 514.5 nm; laser power at the Ag electrode 10 mW;  $E_s$  -0.6 V, 0.1 M KCl and  $10^{-3}$  M  $\text{Na}_2\text{HPO}_4$ ; pH 8; cytosine concentration  $1 \times 10^{-3}$  M. (Lewinsky, Ref. <sup>39</sup>).

NRS spectrum of cytosine (below). Conditions: laser excitation line 514.5 nm; laser power 120 mW;  $10^{-2}$  M cytosine in  $\text{H}_2\text{O}$ ; accumulation time  $2 \text{ s/cm}^{-1}$ ; 6 scans

is about  $30 \text{ cm}^{-1}$ . Therefore, the previously assigned vibrational bands of the NSRS spectra can be compared with the SERS spectra. The enhancement factor of the inplane ring; breathing mode of cytosine at  $800 \text{ cm}^{-1}$  is about  $10^6$ . With a polished and chemically cleaned silver electrode a strong Raman signal from the vibrational lines of a biomolecule appears only after an electrochemical oxidation reduction cycle, a so-called "activation cycle". Such a cycle consists of:

1) The oxidation of the Ag electrode  $\text{Ag}^0 \rightarrow \text{Ag}^+ + \text{e}^-$  where the amount of Ag oxidation is monitored by the total charge passed through the electrode.

2) During the reduction half cycle, a roughened silver surface is reformed by  $\text{Ag}^+ + \text{e}^- \rightarrow \text{Ag}^0$ . Scanning electron microscopy (SEM) of electrode surfaces after this oxidation-reduction procedure have revealed that the initially smooth surfaces have acquired bumps on the scale of 25 to 500 nm<sup>8</sup>. These bumps can be approximated as spheres, hemispheres and prolate spheroids<sup>8</sup>.

This "SERS active" surface consists of randomly distributed surface bumps with a surface topography in the 25 nm region (conventional SEM resolution range), the submicroscopic size range (2–20 nm) and even in the atomic scale roughness from a single atom to 2 nm. These structures produce large electromagnetic fields on the surface when the incident photon energy is in resonance with the localized surface plasmons (submicroscopic spheres and spheroids) and the single atoms or clusters enhance the Raman polarizability (cf. Chapt. 3).

Recently, two small-volume electrochemical cells for the measurements of surface enhanced Raman scattering of very small amounts of biological material were developed<sup>33</sup>. The mini-SERS cell (cf. Fig. 2b) with a volume of about 0.8 ml is used

for a normal Raman spectrometer and the angle between the incoming laser beam and the electrode surface can be chosen. The minicell consists of a brass frame and a Teflon inner part. The silver working electrode with a diameter of 3 mm is fitted into a Teflon rod which can be inserted from the back of the cell.

The cell design shown in Fig. 2c has been used for micro-SERS spectroscopy of chromosomes and related material <sup>36)</sup>. This microcell is for use in a Raman microspectrometer using epi-illumination. By choice of the objective used in the microscope, the focus of the laser beam is about 6  $\mu\text{m}$  in diameter for a typical chromosome micro-SERS-spectrum. The working electrode, with a diameter of 0.5 mm, is fitted into a perspex rod and can be screwed into a frame for positioning the electrode surface to the objective of the microscope. This small microcell needs only 0.08 ml of sample.

## 2.2 Colloid SERS

Metal colloids in an aqueous solution are ideal markers for cell surfaces and intracellular components for microscopic observation (light and fluorescence microscopy, transmission and scanning electron microscopy) and for studying molecular organization and cell function <sup>104)</sup>. It also has numerous medical uses as a drug and as a test for various diseases <sup>105)</sup>. For more specific information about the interfacial behaviour of biomolecules adsorbed on metal colloids several studies of complex molecules by means of colloid SERS- <sup>25,27,41)</sup>, and SERRS spectroscopy <sup>22,106)</sup> have been published. This is an application of metal colloids which may become of great practical value, particularly in the vibration spectroscopy of biomolecules in the adsorbed state. The advantage of this colloid SERS spectroscopy is the simple experimental pretreatment procedure and the Raman measurements in conventional liquid cells or in capillaries. An additional advantage as compared with the electrode SERS spectroscopy is that the molecular structure is not influenced through the oxidation-reduction cycle during pretreatment.

The silver colloids are prepared according to Creighton et al. <sup>69)</sup>. They are formed by rapidly mixing a solution of  $\text{AgNO}_3$  with icecold  $\text{NaBH}_4$ . This aggregated sols exhibit visible absorption spectra in which the 390 nm peak is attributable to small particle resonant Mie scattering <sup>70)</sup>. This yellow unaggregated colloid is stable for several weeks. Transmission electron microscopy shows that these colloids consist of 7 to 15 nm average diameter faceted crystals <sup>82)</sup>. The addition of a solution containing a biomolecule leads to a decrease in the main absorption band of the hydrosol at 380–390 nm and to the appearance of long-wavelength bands (cf. Fig. 4). These long-wavelength bands originate from aggregates of silver micelles formed during the adsorption process. The electron microscopic analysis of the hydrosol-phenylalanine complex (Phe) has shown that the silver micelles form aggregates of about 150–200 nm in diameter <sup>27)</sup>.

Aggregation of the colloid is a required first step to obtain SERS spectra of adsorbed molecules <sup>76,79)</sup>. This aggregation can be initiated by adding negatively charged ions ( $\text{Cl}^-$ ,  $\text{ClO}_4^-$ ,  $\text{NO}_3^-$ ). A SERS spectrum occurs when the negatively charged species are displaced from the silver surface by more strongly bound adsorbates with the rate determined by the nature and concentration of the displacing species <sup>92)</sup>. Weitz et al.

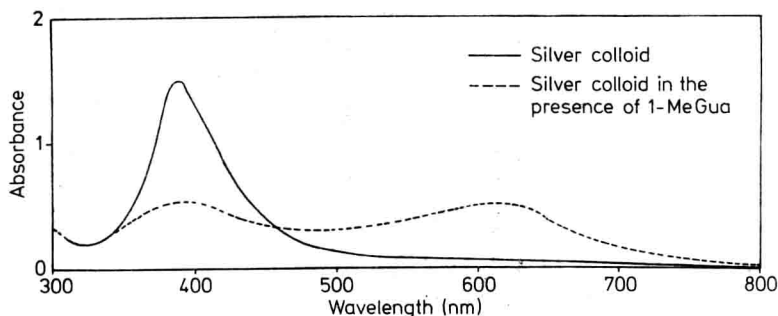


Fig. 4. Absorption spectra of silver sol (solid line) and silver sol in presence of 1-MeGua ( $7 \times 10^{-6}$  M of 1-MeGua)

have reported useful informations about the structure of colloidal aggregates, kinetics of aggregation and theoretical developments<sup>93)</sup>.

The disadvantage of the colloid system is its tendency to flocculate and precipitate at the bottom of the spectroscopic cell. It was recently demonstrated that this annoyance can be avoided by application of the silver colloidal hydrosols on filter paper<sup>107)</sup>, chromatographic paper<sup>108)</sup> and silica gel plates<sup>109)</sup>. With this new technique, subnanogram amounts of various dyes<sup>107)</sup> and nonresonant biomolecules<sup>109)</sup> were detected. It was found that the aggregated Ag sols (i.e. colloidal silver metal particles with adsorbed biomolecules) exhibited strong SER scattering of incident light in the blue-green region. The excitation profile investigations of an amino acid-Ag-sol complex have shown that the excitation maximum of the complex coincides well with the maximum of the long-wavelength absorption band<sup>27)</sup>. Moreover, the shift of the absorption band maximum at increased concentrations of the amino acid (Phe) was accompanied by the same shift in the excitation maximum<sup>27)</sup>.

The SERS spectra of 9-methylguanine (-9MeGua) in Fig. 5 demonstrate the high sensitivity of the colloid SERS technique. The normal Raman spectrum (Fig. 5a) could only be obtained at a rather high concentration of  $10^{-2}$  M and a laser power of 300 mW. The characteristic ring-breathing mode is located at  $634\text{ cm}^{-1}$  and two skeletal vibrations were observed at  $1374\text{ cm}^{-1}$  and  $1410\text{ cm}^{-1}$ . The broad band at  $1634\text{ cm}^{-1}$  is attributed to the water H—O—H bending mode and this band almost blurs the typical guanine vibrations in this spectral region.

The SERS spectra of 9-MeGua in the presence of Ag sol particles are shown in Fig. 5c. The SERS is so sensitive that the concentration could be reduced to  $7 \times 10^{-7}$  M, although the laser power is only 120 mW. The most characteristic features of this spectrum are located at  $660\text{ cm}^{-1}$  and  $1338\text{ cm}^{-1}$  and are due to the guanine ring-breathing mode and a skeleton vibration. In addition, one notes that the water bending vibration is not enhanced and the guanine vibrations now stand out clearly in this spectral range.

Figure 5d demonstrates the subnanogram detection of 9-MeGua (nonresonant in the visible region) on silica gel plates used for thin layer chromatography.  $1\text{ }\mu\text{l}$  ( $125 \times 10^{-12}$  g) of the 9-MeGua colloid complex was applied to the silica gel plate and the plate spot (2 mm in diameter) was then investigated with a typical  $90^\circ$  Raman scatter-

ing arrangement. Using this technique, subnanogram amounts of various methylated guanine derivatives were detected and identified directly with the colloid SERS spectroscopy<sup>109)</sup>. To the knowledge of the authors, this was the first application of SERS in biochemistry for the *in situ* detection and identification at subnanogram levels.

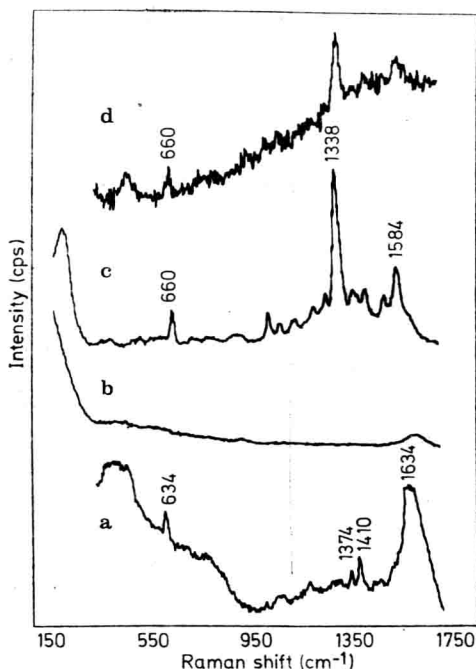


**Fig. 5a-d.** NRS and SERS spectra of 9-methylguanine (9-MeGua); 514.5 nm excitation, monochromator slit width 5 cm<sup>-1</sup>.  
**a)** NRS spectrum of 9-MeGua, 10<sup>-2</sup> M in 0.5 M HCl. Laser power 300 mW; accumulation time 3 s/cm<sup>-1</sup>; 5 scans;  
**b)** SERS spectrum of silver colloid solution (blank spectrum). Laser power 120 mW; accumulation time 2 s/cm<sup>-1</sup>; 1 scan;  
**c)** SERS spectrum of silver colloidal aggregate solution with 9-MeGua, 7 × 10<sup>-7</sup> M at pH 5. Laser power 120 mW; accumulation time 2 s/cm<sup>-1</sup>; 1 scan;  
**d)** SERS spectrum of solution c) applied on HPTLC silica gel plate (120 pg of 9-MeGua). Laser power 120 mW; accumulation time 2 s/cm<sup>-1</sup>; 3 scans

### 3 Characteristics of SERS

#### 3.1 Raman Scattering of Adsorbates

The purpose of this section is to provide some background to the theories by introducing theoretical expressions for Raman scattering intensities and outlining some of the more important features of the various theories: "classical" electromagnetic enhancement (EM enhancement) and "nonclassical" contributions (chemical effects).

The intensity of a Raman line corresponding to a transition between an initial state, *i*, and a final state, *f*, is given by<sup>110)</sup>:

$$I_{fi} = I_{fi}(\omega_s) = \frac{2^3 \pi}{3^2 c^4} \omega_s^4 I_L \sum_{\mathbf{q}, \sigma} |\alpha_{fi}^{\mathbf{q}\sigma}|^2 \quad (1)$$

where  $\omega_s = 2\pi c \bar{\nu}_s$  (in cm<sup>-1</sup>) is the frequency of the scattered light,  $\omega_s = \omega_L - \omega_R$ ;  $\omega_L$ : incident laser frequency;  $\omega_R$ : Raman active normal mode excited by the inelastic

scattering process,  $I_L$  is the intensity of the incident laser light,  $\rho$  and  $\sigma$  are the polarizations of the Raman and incident light respectively, and  $\alpha^{\rho\sigma}$  is the  $\rho, \sigma$ th component of the polarizability tensor. Intensities of scattering processes are alternatively expressed in terms of differential cross-sections  $d\sigma/d\Omega$ :

$$\Omega \frac{d\sigma(\omega_s)}{d\Omega} = \frac{2^3\pi}{3^2c^4} \omega_s^4 \sum_{\rho, \sigma} |\alpha_{fi}^{\rho\sigma}|^2 \quad (2)$$

so that  $I_{fi}$  becomes

$$I_{fi} = \Omega \frac{d\sigma}{d\Omega} I_L \quad (3)$$

The Raman scattering tensor  $\alpha_{fi}$  is

$$\begin{aligned} \alpha_{fi}^{\rho\sigma} = \sum_e & \frac{\langle \psi_f | \underline{e}_\rho \mu | \psi_e \rangle \langle \psi_e | \underline{e}_\sigma \mu | \psi_i \rangle}{(E_e - E_i) - \hbar\omega_L + i\Gamma_e} \\ & + \frac{\langle \psi_f | \underline{e}_\sigma \mu | \psi_e \rangle \langle \psi_e | \underline{e}_\rho \mu | \psi_i \rangle}{(E_e - E_f) + \hbar\omega_L + i\Gamma_e} \end{aligned} \quad (4)$$

where  $\mu$  is the dipole moment operator, and  $\underline{e}_\rho$  and  $\underline{e}_\sigma$  are the scattered and laser polarization vectors.  $\psi_e$  represents an intermediate state in the Raman scattering process.  $E_i$  is the initial energy and  $E_f$  the final energy.

The normal Raman scattering (NRS) regime is defined by the condition  $\hbar\omega_L \ll (E_e - E_i)$ . Resonance Raman scattering (RRS) is defined by the condition  $\hbar\omega_L \approx (E_e - E_i)$ . In RRS the value of  $d\sigma/d\Omega$  corresponding to the by resonance enhanced value of  $\alpha_{fi}^{\rho\sigma}$  can be  $10^2$  to  $10^6$  times greater than in the corresponding NRS case.

In 1977 two groups, Jeanmaire and Van Duyne<sup>43)</sup> and Albrecht and Creighton<sup>45)</sup> showed that the Raman cross section for pyridine adsorbed onto electrochemically roughened silver electrodes was enhanced  $10^6$  times:

$$\{I_{fi}(\omega_s)\}_{ads} \approx 10^6 \{I_{fi}(\omega_s)\}_{free} \quad (5)$$

There is some experimental evidence to indicate that much of the enhancement is associated with surface roughness (local microstructures) in the range of 1 to 100 nm. At resonance with these microparticle modes the local electric field at the incident frequency ( $\hbar\omega_L$ ) becomes large near and on the particle surface. Furthermore, the re-radiation efficiency of Raman active molecules situated near the surface also becomes enhanced when the inelastically scattered frequency ( $\hbar\omega_s$ ) is also in resonance with these microparticle modes. The Raman scattering intensity of the adsorbed molecule is then given by<sup>8)</sup>

$$\{I_{fi}(\omega_s)\}_{ads} = I_L(\omega_L) \cdot L^2(\omega_L) \cdot L^2(\omega_s) \cdot \Omega \cdot \left( \frac{d\sigma_{eff}}{d\Omega} \right)_{ads} \cdot N_{sur} \quad (6)$$

Here,  $L^2(\omega_L) \cdot L^2(\omega_s)$  describes the electromagnetic surface-averaged intensity enhancement factors at the incident and Stokes Raman frequencies, respectively

(i.e. the “classical” enhancement by surface plasmon type resonance).  $(d\sigma_{\text{eff}}/d\Omega)_{\text{ads}}$  takes into account a “chemical” effect due to electronic interaction between the chemisorbed molecule and the surface.  $N_{\text{sur}}$  is the number of adsorbed molecules.

The dominant mechanism seems to be the EM effect with enhancements approximately estimated to be in the range of  $10^4$  to  $10^6$ . The chemical mechanisms appear to contribute a combined factor in the range from 10 to  $10^2$ .

### 3.2 The EM Model for SERS

The basic concept of the purely electro-magnetic model considers a Raman active molecule (scatterer) near a metallic particle<sup>111–126</sup> and is shown schematically in Fig. 6. The main features of these theories are seen by considering a single dielectric ellipsoid with a laser excitation field  $E_L(\omega_L)$  directed along the principal axis of the ellipsoid. Then the field  $E_{ins}$  inside the particle is uniform and given by<sup>140</sup>:

$$E_{\text{ins}}(\omega_L) = \frac{\epsilon_s}{\epsilon_s + (\epsilon_m - \epsilon_s) A_c} E_L(\omega_L) \quad (7)$$

Here  $\epsilon_m$  and  $\epsilon_s$  denote the dielectric functions of the metallic sphere and its surrounding, respectively.  $A_c$  is a depolarization factor depending solely on particle shape.

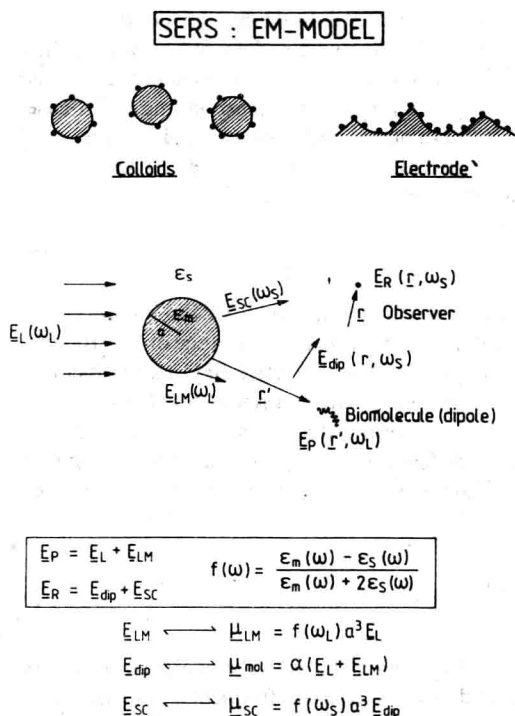


**Fig. 6.** Schematic picture indicating the origins for the EM-enhancement



$\varepsilon_m(\omega) = \varepsilon_1(\omega) + i\varepsilon_2(\omega)$  is the expression for the complex dielectric constant. The maximum of the internal field  $E_{\text{ins}}$  occurs at a frequency  $\omega_{\text{sp}}$ , where

$$\varepsilon_1(\omega_{\text{sp}}) \approx (1 - 1/A_c) \varepsilon_s \quad (8)$$

The condition corresponds to the excitation of localized surface plasmons. Silver can satisfy this condition for visible light.

The expression (7) for  $E_{\text{ins}}$  is identical to that of the electric field, due to an ideal dipole at the center of the sphere ( $A_c = 1/3$ )

$$\mu(\omega_L) = \alpha E = \frac{\varepsilon_m(\omega_L) - \varepsilon_s(\omega_L)}{\varepsilon_m(\omega_L) + 2\varepsilon_s(\omega_L)} a^3 E_L \quad (9)$$

The general elastically scattered field of the sphere is calculated by the Lorenz-Mie theory<sup>128)</sup> and is denoted  $E_{\text{LM}}(r', \omega)$ .

Considered is a Raman scattering molecule located at coordinate  $r'$  outside of a spherical particle of radius  $a$ . If the electromagnetic wave of frequency  $\omega_L$  is incident on that small sphere, the total field outside the sphere is equivalent to  $E_L(r', \omega_L)$  plus the field  $E_{\text{LM}}(r', \omega_L)$ . This field polarizes the molecule and induces a dipole moment.

$$\mu_{\text{mol}} = \alpha_{\text{mol}} \{E_L(r', \omega_L) + E_{\text{LM}}(r', \omega_L)\} = \alpha_{\text{mol}} E_p(r', \omega_L) \quad (10)$$

The electric field of this dipole  $\mu_{\text{mol}}$  is  $E_{\text{dip}}(r', \omega_s)$  for the observer at  $r$ . Beside this direct radiation, the vibrating molecule also polarizes the metal sphere and uses it as an antenna to amplify its Raman radiation.

$E_{\text{dip}}$  induces a dipole  $\mu_{\text{sc}}$  in the metal particle with the radius  $a$

$$\mu_{\text{sc}}(\omega_s) = \frac{\varepsilon_m(\omega_s) - \varepsilon_s(\omega_s)}{\varepsilon_m(\omega_s) + 2\varepsilon_s(\omega_s)} a^3 E_{\text{dip}} \quad (11)$$

In the dipole approximation, the field outside the sphere ( $E_{\text{sc}}$ ) is the same as that generated by this dipole. The electric field at the observer  $r$  is

$$E_R = E_{\text{dip}} + E_{\text{sc}} \quad (12)$$

The calculated enhancement of this purely physical EM effect as function of the distance of the molecule from the sphere, reflects the long range nature of this model<sup>112)</sup>. The enhancement depends strongly upon the particle shape and the dielectric constants  $\varepsilon_m$  and  $\varepsilon_s$ <sup>113,127)</sup>. For small spheres, in resonance with the localized surface plasmons, the local field strength averaged over the surface is about 1000 times the incident field strength. Detailed calculations for isolated prolate ellipsoids have been reported<sup>122,123)</sup>. It seems clear that even more calculations exploring the limits of these electro-magnetic effects are needed in order to compare the experimental results with this EM model.